

Parametrization of 2-Bromo-2-Chloro-1,1,1-Trifluoroethane (Halothane) and Hexafluoroethane for Nonbonded Interactions

Zhanwu Liu,[†] Yan Xu,^{†,‡} Alexander C. Saladino,[†] Troy Wymore,[§] and Pei Tang^{*,†,‡}

Departments of Anesthesiology and Pharmacology, University of Pittsburgh School of Medicine, Pittsburgh, Pennsylvania 15261, and Pittsburgh Supercomputing Center, Biomedical Initiative Group, 4400 Fifth Avenue, Pittsburgh, Pennsylvania 15213

Received: September 24, 2003; In Final Form: November 19, 2003

Ab initio and empirical methods were combined to optimize the partial atomic charges and Lennard-Jones parameters for two halogenated compounds, halothane (CF_3CHClBr , a potent volatile anesthetic) and hexafluoroethane (CF_3CF_3 , a nonanesthetic). Charge optimization was achieved using empirical calculations by systematically adjusting the charge assignments to fit minimum interaction energies and geometries between a TIP3 water molecule and the halogenated compounds to the corresponding values from the ab initio calculations, which were carried out at the HF/6-311+G(2d,p) and HF/6-31G(d) levels for halothane and hexafluoroethane, respectively. To optimize the Lennard-Jones parameters, the initial estimates were obtained from scaling the values from the ab initio minimum interaction energies and geometries between neon and the halogenated compounds calculated at the MP3/6-311++G(3d,3p) level. The Lennard-Jones parameters were further refined by fitting the empirical interaction energies to the corresponding ab initio values. The refined parameters were finalized by reproducing experimental values of the heats of vaporization and densities for liquid halothane and hexafluoroethane, using molecular dynamics simulations. The calculated heats of vaporization and liquid densities using the optimized parameters are in excellent agreement with the experimental values. The results indicate that the combination of ab initio and empirical approaches works well for obtaining the nonbonded parameters of molecules with heavy halogen atoms, such as Cl and Br. The refined nonbonded parameters are readily applicable in molecular dynamics simulations involving these halogenated compounds.

Introduction

Many halogenated compounds, such as halothane (CF_3CHClBr), are potent general anesthetics whose potencies correlate strongly with their solubility in olive oil, as predicted by the so-called Meyer–Overton rule.^{1,2} Other halogenated compounds, particularly perfluorinated compounds such as hexafluoroethane (C_2F_6), are structurally similar to general anesthetics and predicted by the Meyer–Overton rule to be potent anesthetics but produce no anesthesia.³ The molecular properties differentiating these two classes of compounds are only vaguely defined.^{4,5} Because the molecular mechanisms of general anesthesia are still poorly understood, a systematic comparison and use of novel anesthetic–nonanesthetic (or, more precisely, nonimmobilizer) pairs will shed new light on the molecular characteristics that set the anesthetics as one class apart from the nonanesthetics as another.

The need for a better understanding of the molecular properties of halogenated compounds becomes even more apparent when the interactions of these molecules with their potential targets (e.g., membrane proteins) are under investigation by molecular modeling. Computational approach to delineating drug effects on membrane proteins has become amenable

with the development of the state-of-the-art parallel computing and the optimization of the force fields for lipids and proteins. Specifically, molecular dynamics (MD) simulations can provide molecular details of the effects of anesthetics on ion channel structure and dynamics,⁶ revealing underlying molecular processes that are of functional importance to general anesthesia.

A problem frequently encountered in using MD simulations to study drug effects on proteins is the lack of reliable force field parameters for the halogenated drug molecules, despite the great efforts being devoted to improving the accuracy of force field parameters in general for the past decades.^{7–15} One common solution is to use parameters from similar molecules or submolecular groups. Sometimes this method is successful, especially for bond and angle parameters, but it can often introduce significant errors in the simulations. Among all force field parameters, Lennard-Jones (LJ) parameters and atomic charges are usually designed for quantifying dispersion–attraction and electrostatic interactions, respectively. Because these nonbonded interactions are responsible for many chemical and biological properties of the drug molecules, it is of vital importance to derive robust nonbonded parameters for accurate characterization of the nonbonded interactions between drugs and their potential biological targets.

Ab initio calculations of the nonbonded interactions in dimeric molecule complexes have been reviewed recently, with discussions on how the theory levels and basis sets affect the basis set superposition error (BSSE).¹⁶ It is suggested that the MP3/6-311++G(3d,3P) level of theory without BSSE correction is appropriate for the calculation of relative interaction energies and complex geometries when helium or neon is used as a probe

* Author to whom correspondence may be addressed. W-1357 Biomedical Science Tower, University of Pittsburgh School of Medicine, Pittsburgh, PA 15261. Tel: (412) 383-9798. Fax: (412) 648-9587. E-mail: tangp@anes.upmc.edu.

[†] Department of Anesthesiology, University of Pittsburgh School of Medicine.

[‡] Department of Pharmacology, University of Pittsburgh School of Medicine.

[§] Pittsburgh Supercomputing Center.

for the van der Waals surfaces of molecules.¹⁷ A combined ab initio/empirical approach has been developed recently,^{18,19} in which relative values of the LJ parameters are determined by mirroring the trends in the ab initio calculated minimum interaction energies and geometries between a rare gas atom and the model compound. The absolute values are then determined by reproducing the experimental pure liquid properties, such as the heat of vaporization and density, of these compounds. The LJ parameters of alkanes¹⁸ and the partial atomic charges and LJ parameters of fluoroethanes and amines¹⁹ have been optimized using this approach, suggesting that generalization of this method might be applicable to other halogenated compounds containing heavy atoms.

In the present study, we examined the validity of using the combined ab initio/empirical approach to optimizing the nonbonded parameters of halothane and hexafluoroethane. It is generally realized that parametrization becomes more challenging with compounds having heavy halogen atoms (e.g., Cl and Br in halothane) because of the more polarizable nature of these atoms. Therefore, the choice of halothane provides a critical test of the new parametrization method. The strength and limitation of the combined ab initio/empirical approach are revealed in the present study, providing a basis for the further refinement of this approach. It is believed that the resultant parameters, made fully compatible with the CHARMM force field, are superior to those of the similar compounds in the existing force field for MD simulations of anesthetic and nonimmobilizer effects on proteins.

Methods

The combined ab initio and empirical parametrization method, detailed in the literature,¹⁹ was used to determine the partial atomic charges and LJ parameters of halothane and hexafluoroethane. Briefly, after the geometry of individual halogenated compounds was optimized, three different types of calculations were performed to optimize the nonbonded parameters: (1) Ab initio calculations were used to obtain the interaction energy profiles and geometries of dimers formed by the halogenated molecules with nonpolar neon or polar water in the gas phase. The results of these ab initio calculations were used as the target data for parameter adjustments in the subsequent steps of the empirical calculations. (2) The empirical method was employed to adjust and optimize partial atomic charges or the ratio of the LJ parameters by reproducing both the minimum interaction energies and geometries of the drug–water or drug–neon dimers, respectively. (3) MD simulations in the condensed phase were performed to refine the LJ parameters by comparing the density and the heat of vaporization with the corresponding experimental values. Steps (2) and (3) were iterated until agreement with ab initio and experimental results were simultaneously achieved.

Ab Initio Calculations. The Gaussian 98 program²⁰ was used for all ab initio calculations. Geometry optimizations and preliminary partial atomic charge assignments of hexafluoroethane were carried out in the same fashion as for halothane,⁷ using the hybrid B3LYP density-functional theory (DFT) method^{21,22} with two different basis sets, 6-31G(d) and 6-311+G(2d,p).^{23–25} Neon or water was paired with all non-equivalent atoms in halothane or hexafluoroethane for the calculations of nonbonded interactions. Several representative orientations of pairing are shown in Figure 1. By (1) varying the interaction distance systematically between neon and a given atom in a particular complex, (2) calculating single-point energy of the complex and the energy differences between the complex

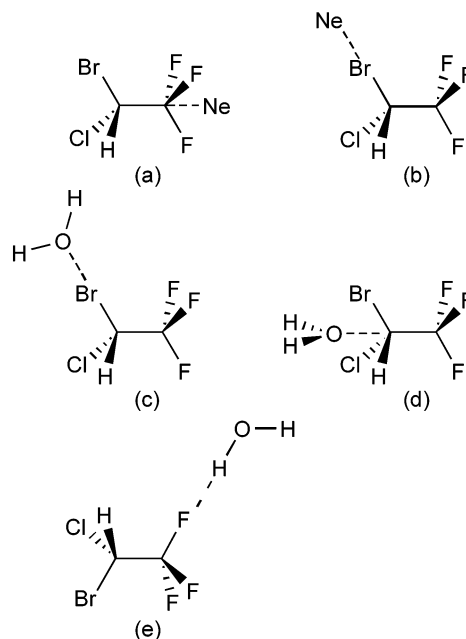


Figure 1. Interaction orientations between halogenated molecules (halothane as shown) and neon atom (a and b) or water molecule (c, d, and e). See Tables 2–4 for the calculated parameters.

and the corresponding monomers, and (3) repeating such calculations for several possible complex orientations, we have derived the interaction energy profiles of the halothane–neon and the hexafluoroethane–neon complexes at the MP3/6-311++G(3d,3p) level using the third-order Møller–Plesset theory.^{26,27} In a similar way, minimum-interaction energies and distances of hexafluoroethane or halothane with TIP3 water²⁸ were determined at the HF/6-31G(d) or HF/6-311+G(2d,p) levels, respectively. The results were used as “the targets” for the later empirical calculations.

Empirical Calculations using CHARMM. The TIP3 water model with Charmm27 force field was used in the empirical calculations. LJ parameters and charges were optimized using the CHARMM27b1 software package^{8,29} on a SGI Octane workstation. The optimization procedure is similar to the methodology developed by Chen et al.¹⁹ Interaction energy surfaces were determined by calculating the differences between the complex energy and the sum of the isolated monomer energies when the interaction distance was systematically increased. The results from CHARMM and the ab initio calculations were compared with only the Coulomb and LJ 6–12 terms included in the energy surface from the CHARMM calculations. The LJ parameters and partial atomic charges were adjusted iteratively to reach the minimum root-mean-square (RMS) fluctuation of the difference between the ab initio and the empirical results.¹⁸

Because of the involvement of the polarizable heavy halogen atoms in halothane, the dipole moment was used as an additional criterion to judge the acceptability of the resulting parameter sets. The dipole moment of an isolated halothane, measured in the condensed phase in a diluted CCl₄ solution at 298.15 K,³⁰ is 1.41 D. This experimental value served as a good reference point for charge optimizations. The charge sets that either had obvious unreasonable charge distribution (e.g., C being much more negative than F) or generated dipole moments greatly deviating from the reference value of 1.41 D were not considered in the further refinements.

Refinement of LJ Parameters by Molecular Dynamics Simulations. LJ parameters of both compounds were further

refined in MD simulations using the NAMD2 program (version 2.5)³¹ on the Cray T3E at the Pittsburgh Supercomputing Center. To predict the pure solvent properties, 216 hexafluoroethane molecules were generated with random positions and orientations in a $32 \times 32 \times 32 \text{ \AA}^3$ cubic box so that the initial liquid density at 195 K agreed with the experimental value of 1.59 g/mL.³² Similarly, the same number of halothane molecules were generated in a cubic box of $34 \times 34 \times 34 \text{ \AA}^3$ for the initial liquid halothane density of 1.86 g/mL at 298 K.³³ Simulations in the gas phase were performed with eight molecules in cubic boxes having sides of 60 and 68 Å for hexafluoroethane and halothane, respectively.

The molecular energy was calculated from the sum of the bond stretching, bond bending, torsion angle, and nonbonded terms. The parameters for all energy terms, except for the nonbonded term, were adopted from the CHARMM22 force field.⁸ The bonded interactions were calculated for each time step at 1 fs/step. The short-range nonbonded interactions, including the van der Waals and electrostatic interactions, were computed every two time steps. The long-range electrostatic interactions were evaluated using the particle mesh Ewald method³⁴ with periodic boundary conditions. A smooth splitting function at a switch distance of 8.5 Å was used to truncate the van der Waals potential energy. The cutoff distance for the nonbonded interactions was 10 Å with the pair list distance extended to 11.5 Å.

Simulations for each liquid box consisted of at least 10 000 steps of energy minimization using a conjugate gradient and line-search algorithm. Each system was equilibrated at constant volume (NVT) for 100 000 steps, and the well-equilibrated system was simulated for 200 000 steps (200 ps) with fully flexible cells at the constant pressure and constant temperature (NPT), using the Nosé–Hoover pressure and temperature control^{35,36} with periodic boundary conditions applied. Similar procedures were employed for the simulations in the gas phase except that the ratios of the three dimensions were kept at constant. The total energies collected during the last 120 000 steps of simulations were averaged (E_{liq} or E_{gas}) for the calculations of the heat of vaporization.

For each molecule, the LJ parameters were refined with iterative simulations until the simulated density and the heat of vaporization were within 2.5% of the experimental values. The heat of vaporization was evaluated using eq 1 based on the simulation-generated E_{gas} and E_{liq} values

$$\Delta H_{\text{vap}} = E_{\text{gas}} - E_{\text{liq}} + RT \quad (1)$$

The local structures of halothane and hexafluoroethane in the liquid phase and the interactions of halothane with bulk water were evaluated by radial distribution functions (RDFs). A single halothane molecule was placed in the center of a cubic box ($23 \times 23 \times 23 \text{ \AA}^3$) of 393 TIP3 water molecules, and a MD simulation of this halothane–water system was performed under NPT for 200 ps after the system was well equilibrated.

Results and Discussion

Halothane geometry was optimized in our previous study⁷ at the B3LYP/6-311+G(2d,p) level. Staggered and eclipsed conformations of hexafluoroethane were studied previously by other groups.^{37,38} In the present study, we used the same DFT method and basis set as for halothane to optimize the staggered hexafluoroethane conformation, which should be the dominate conformation in reality. A reduced basis set 6-31G(d) was also tested based on the consideration that there were no heavy

TABLE 1: Optimized Geometric Parameters of Hexafluoroethane

bond-length angle	B3LYP/6-311+G(2d,p)	B3LYP/6-31G(d)	exp ^a
	C–C (Å)	1.552	1.544
C–F (Å)	1.334	1.338	1.326
<CCF (°)	109.83	109.84	109.8

^a Reference 32.

TABLE 2: Minimum Interaction Energies and Distances of Neon with Hexafluoroethane and Halothane^a

orientation	interaction energies (kcal/mol)		interaction distances (Å)	
	emp	MP3	emp	MP3
Hexafluoroethane				
C–Ne	−0.31	−0.74	3.4	3.3
F–Ne	−0.16	−0.53	3.1	2.9
Halothane				
C _r –Ne	−0.40	−0.75	3.4	3.3
F–Ne	−0.23	−0.61	3.0	2.9
C–Ne	−0.42	−0.53	3.7	3.9
Br–Ne	−0.19	−0.53	3.6	3.4
Cl–Ne	−0.19	−0.58	3.5	3.3
H–Ne	−0.29	−0.91	2.6	2.4

error analysis	energetics		distances	
	difference	ratio	difference	ratio
Hexafluoroethane				
average	0.40	0.36	0.2	1.05
RMSF	0.03	0.06	0.0	0.00
Halothane				
average	0.36	0.45	0.2	1.03
RMSF	0.15	0.17	0.1	0.04

^a See Figure 1 for interaction orientations. emp: empirical calculation by CHARMM. MP3: MP3/6-311+G(3d,3p). See ref 18 for error analysis. RMSF: root-mean-square fluctuation.

atoms, such as Br or Cl, involved in hexafluoroethane. As shown in Table 1, the influence of basis sets on the bond lengths and angles was minute. The deviations between the calculated and the experimental values were well within 1%. The geometric parameters of hexafluoroethane were also in excellent agreement with the results obtained by others.^{37,38} The optimized conformation of hexafluoroethane at the B3LYP/6-311+G(2d,p) level was used in subsequent calculations in this study.

Table 2 summarizes the minimum interaction energies and distances of the neon–hexafluoroethane pairs and the neon–halothane pairs from the empirical and ab initio calculations. The average differences and ratios of the interaction distances for both compounds reveal that empirical distances fit well with the ab initio results, but the minimum–interaction energies with neon mismatch considerably. This discrepancy in the minimum interaction energies between the empirical and ab initio calculations was also observed previously when neon was used as a probe for other molecules and was attributed mainly to the omission of the BSSE correction.¹⁸ Nevertheless, the relative orders of the interaction energies between neon and various atoms in the halogenated molecules are reasonably reserved in this study so that the present methodology has certain merit for LJ parametrizations. The omission of the BSSE correction in the present method was to prevent outward shifts in the position of minimum interaction distances observed in the ab initio calculations. It is worth noting that poor condensed-phase properties were observed when the BSSE correction was included in the calculations at the MP3/6–311(3d, 3p) level for methane.³⁹

TABLE 3: Minimum Interaction Energies and Distances of Water with Hexafluoroethane^a

orientation	interaction energies (kcal/mol)		interaction distances (Å)	
	emp	HF	emp	HF
C–OH ₂	−0.65	−1.23	3.56	3.29
F–HOH	−0.69	−0.55	2.04	2.47

error analysis	energetics		distances	
	difference	ratio	difference	ratio
average	0.36	0.89	0.35	0.95
RMSF	0.22	0.36	0.08	0.13

^a HF calculations were at the HF/6-31G(d) level. RMSF: root-mean square fluctuation.

TABLE 4: Minimum Interaction Energies and Distances of Water with Halothane

orientation	interaction energies (kcal/mol)			interaction distances (Å)		
	emp	HF1 ^a	HF2 ^a	emp	HF1	HF2
C _f –OH ₂	−0.08	−0.08	−0.56	3.62	3.65	3.40
F–HOH	−1.61	−0.70	−0.94	1.91	2.57	2.41
C–OH ₂	−1.32	−0.22	−0.68	3.82	4.44	3.79
Br–OH ₂	−0.34	−1.74	−2.99	3.81	3.18	3.07
Cl–OH ₂	−0.15	−1.25	−1.29	3.79	3.20	3.16
H–OH ₂	−2.63	−4.00	−4.74	2.52	2.26	2.15

error analysis ^b	energetics		distances	
	difference	ratio	difference	ratio
average	0.98	1.71	0.47	1.02
RMSF	0.47	2.05	0.24	0.17

^a HF1 and HF2 calculations were at the HF/6-311+G(2d,p) and HF/6-31G(d) levels, respectively. ^b The results of HF1 were used.

It is conceivable that a higher-level function with more computational cost for ab initio calculations might reduce the size of mismatching between the minimum interaction energies from the empirical and ab initio calculations. Such exercises, however, may prove unnecessary. As pointed out by Chen et al.,¹⁹ the assumptions in the use of the combined ab initio/empirical approach are that the data from ab initio can yield a correct relative ordering of minimum interaction energies and distances, and the relative ordering can be used as one of the restraints to generate the relative values of the LJ parameters and to reduce some randomness in the parameter sets that satisfy condensed-phase properties. After all, the finalized LJ parameters will be generated from the proportional scaling in the condensed-phase simulations.

The minimum interaction energies and distances of TIP3 water with hexafluoroethane and halothane are listed in Tables 3 and 4, respectively. Because halothane contains two heavy halogen atoms of the third and fourth row (Cl and Br), ab initio calculations were performed at both the HF/6-311+G(2d,p) level (HF1) and HF/6-31G(d) level (HF2), whereas only the latter was used for hexafluoroethane. Two additional restraints were applied for the adjustment of the charge values in the empirical calculations: (1) that the initial charge values were scaled from the previous ab initio charges calculated for an isolated halothane;⁷ and (2) that the experimental dipole moment of 1.41 D for an isolated halothane in the condensed phase³⁰ was used as a reference value. Similar to the situation with neon as a probe, the energy profiles exhibited a certain mismatch between empirical and quantum mechanical calculations, as shown in Table 4. Nevertheless, the finalized charges and the optimized LJ parameters for halothane in Table 5 allow for excellent

TABLE 5: Nonbonded Parameters for Hexafluoroethane and Halothane

atom	σ (Å) ^a	ϵ (kcal/mol) ^a	q (e [−])
Hexafluoroethane			
C	3.79	0.039	0.39
F	2.92	0.070	−0.13
Halothane			
C _f	3.53	0.078	0.49
F	2.83	0.098	−0.17
C	3.63	0.055	0.01
Br	3.74	0.314	−0.03
Cl	3.53	0.254	−0.06
H	2.37	0.022	0.10

^a Combination rule: $\sigma_{12} = (\sigma_1 + \sigma_2)/2$; $\epsilon_{12} = (\epsilon_1\epsilon_2)^{1/2}$.

TABLE 6: Condensed-Phase Properties of Hexafluoroethane and Halothane

	ΔH_{vap} (kcal/mol)			density (g/mL)		
	calc	exp ^a	% diff ^b	calc	exp	% diff ^b
Hexafluoroethane						
180 K	4.12	4.04	2.0	1.64	N/A	N/A
195 K	3.87	3.86	0.3	1.58	1.59	−0.6
Halothane						
298 K	6.99	7.08	−1.3	1.84	1.86	−1.1
323 K	6.68	6.71	0.4	1.77	1.73	2.3

^a From ref 41. ^b % diff = ((calc − exp)/exp) × 100.

reproduction of the condensed-phase properties for the compounds, as listed in Table 6. In fact, the differences between the calculated and experimental heats of vaporization and liquid densities using nonbonded parameters in Table 5 are less than 2.5% for both halothane and hexafluoroethane at different temperatures.

A generalized force field for linear, branched, and cyclic perfluoroalkanes was developed previously by fitting the force field results to the conformational profiles from gas-phase ab initio calculations (LMP2/cc-pVTZ(-f)/HF/6-31G*) and to the experimental data for pure liquids.⁴⁰ The transferability of generalized nonbonded parameters (C, $\sigma = 3.50$ Å, $\epsilon = 0.066$ kcal/mol, $q = 0.36$; F, $\sigma = 2.95$ Å, $\epsilon = 0.053$ kcal/mol, $q = -0.12$) of perfluoroalkanes was tested through Monte Carlo statistical mechanics simulations for the pure liquid of hexafluoroethane at 195 K. Although the computed density of the pure hexafluoroethane liquid is in good agreement with the experimental density (1.1% difference), the unsigned error for the heats of vaporization is 3.9%, which is significantly higher than what is obtained (0.3%) at the same temperature in the present study.⁴¹ Compared to the corresponding values in this study, the smaller σ and larger ϵ values for C in the previous study⁴⁰ may be responsible for the larger error in the heats of vaporization. The necessity of increasing σ and reducing ϵ of carbons in hexafluoroethane may arise from the fact, noticed by Nose et al.,⁴² that the direct combination rules and pure liquid LJ parameters often made intermolecular interactions in haloalkanes too attractive.

The local structures of liquid halothane and hexafluoroethane were assessed by intermolecular RDFs. As shown in Figure 2, the closest intermolecular atom–atom contacts between F atoms are, on average, 3.19 Å for halothane and 3.24 Å for hexafluoroethane. RDFs for the center of mass (COM) of molecules reflect average separation of the molecules. The first coordination shell peak of COM–COM RDF for halothane is broader than that for hexafluoroethane and is shifted to the right (larger distances), probably due to the shape of the halothane molecule with heavy atoms having bulky volumes. The first shell peak of the H–H RDFs is well defined for halothane in Figure 2a,

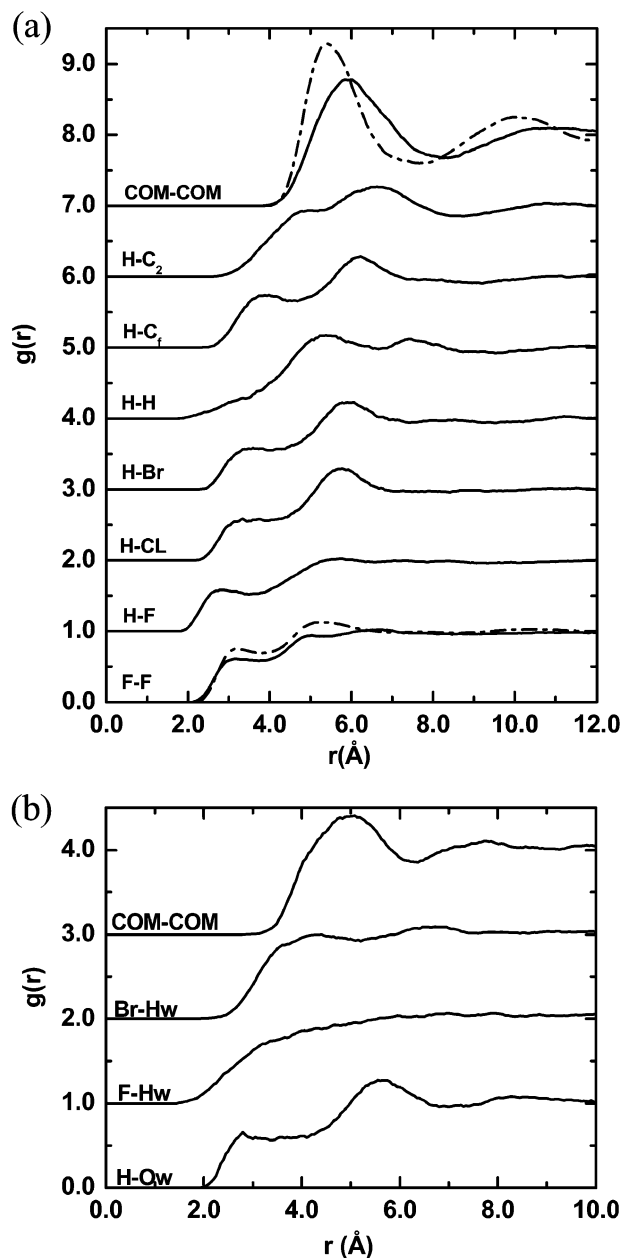


Figure 2. (a) The radial distribution functions $g(r)$ of halothane (solid lines) and hexafluoroethane (dashed lines) and (b) $g(r)$ of halothane with water. The baselines of the curves are offset in 1-unit increments in the y-direction for display clarity.

but the possibility of direct H–H contact seems unlikely with a peak maximum at $\sim 5 \text{ \AA}$. A small but recognizable peak of the H–F RDF in the region of 2.84 \AA reveals possible weak interactions between this pair of atoms, suggesting antiparallel orientations for the immediate neighboring halothane molecules. The first peak maximum for the H–C_f RDF ($r = \sim 3.9 \text{ \AA}$) is smaller than that for H–C RDF ($r = \sim 4.9 \text{ \AA}$), another indication that antiparallel orientation is favorable in the liquid halothane. Indeed, we have observed that two halothane molecules can form an antiparallel pair during our previous MD simulations in a gramicidin–DMPC system.⁶ The antiparallel orientation partially cancels the dipole moment from the individual halothane molecules, causing the pair to have virtually zero dipole moment. It has long been found that permanent or induced dipole moments are necessary for anesthetic action.⁴³ A pair of halothane molecules with virtually no dipole moment prefers the lipid tail region to the lipid–water interface in MD

simulations, making the pairs indistinguishable from nonanesthetic molecules, such as hexafluoroethane.

The behavior of halothane in water was also characterized by RDFs. A small peak of RDF of halothane hydrogen and water oxygen (H–O_w) at $r = \sim 2.8 \text{ \AA}$ in Figure 2b indicates the possibility of weak interactions between these two types of atoms in halothane and water. Both F–H_w RDF and Br–H_w RDF, which is very similar to Cl–H_w RDF (data not shown), reveal that halothane has no well-defined interactions with water at these sites. The COM–COM RDF shows a broad peak at $r = \sim 5 \text{ \AA}$, again reflecting long-range interactions of halothane with water. These results are in good agreement with the fact that halothane has relatively low solubility in water.⁴⁴

In summary, we have optimized nonbonded parameters for hexafluoroethane and halothane. These parameter sets reproduce better condensed-phase properties of these two halogenated compounds than do the previous literature values. The new nonbonded and charge parameters are ready to be implemented in MD simulations.

Acknowledgment. The authors would like to thank Professor Alexander D. MacKerell and Professor Xiaocheng Zeng for stimulating discussions. The research was facilitated through an allocation of advanced computing resources at the Pittsburgh Supercomputing Center through the support of the National Science Foundation and the Commonwealth of Pennsylvania and supported by grants from the NIH (R01GM66358, R01GM56257, and R01GM49202).

Supporting Information Available: The optimized internal geometry of hexafluoroethane is included as supporting material in PDF format. This material is available via the Internet at <http://pubs.acs.org>.

References and Notes

- (1) Meyer, H. H. *Arch. Exp. Pathol. Pharmacol.* **1899**, *42*, 109.
- (2) Overton, E. *Studien uber die Narkose zugleich ein Beitrag zur allgemeinen Pharmacologie*; G. Fischer: Jena, 1901.
- (3) Koblin, D. D.; Chortkoff, B. S.; Laster, M. J.; Eger, E. I., II; Halsey, M. J.; Ionescu, P. *Anesth. Analg.* **1994**, *79*, 1043.
- (4) Xu, Y.; Tang, P.; Liachenko, S. *Toxicol. Lett.* **1998**, *101*, 347.
- (5) Tang, P.; Yan, B.; Xu, Y. *Biophys. J.* **1997**, *72*, 1676.
- (6) Tang, P.; Xu, Y. *Proc. Natl. Acad. Sci. U. S. A.* **2002**, *99*, 16035.
- (7) Tang, P.; Zubryzcki, I.; Xu, Y. *J. Comput. Chem.* **2001**, *22*, 436.
- (8) MacKerell, A. D.; Bashford, D.; Bellott, M.; Dunbrack, R. L.; Evanseck, J. D.; Field, M. J.; Fischer, S.; Gao, J.; Guo, H.; Ha, S.; Joseph-McCarthy, D.; Kuchnir, L.; Kuczera, K.; Lau, F. T. K.; Mattos, C.; Michnick, S.; Ngo, T.; Nguyen, D. T.; Prodhom, B.; Reiher, W. E.; Roux, B.; Schlenkrich, M.; Smith, J. C.; Stote, R.; Straub, J.; Watanabe, M.; Wiorkiewicz-Kuczera, J.; Yin, D.; Karplus, M. *J. Phys. Chem. B* **1998**, *102*, 3586.
- (9) Jorgensen, W. L.; Maxwell, D. S.; Tirado-Rives, J. *J. Am. Chem. Soc.* **1996**, *118*, 11225.
- (10) Wang, W.; Donini, O.; Reyes, C. M.; Kollman, P. A. *Annu. Rev. Biophys. Biomol. Struct.* **2001**, *30*, 211.
- (11) Halgren, T. A. *J. Comput. Chem.* **1996**, *17*, 490.
- (12) Ott, K. H.; Meyer, B. *J. Comput. Chem.* **1996**, *17*, 1068.
- (13) Allinger, N. L.; Chen, K. S.; Lii, J. H. *J. Comput. Chem.* **1996**, *17*, 642.
- (14) Cornell, W. D.; Cieplak, P.; Bayly, C. I.; Gould, I. R.; Merz, K. M.; Ferguson, D. M.; Spellmeyer, D. C.; Fox, T.; Caldwell, J. W.; Kollman, P. A. *J. Am. Chem. Soc.* **1995**, *117*, 5179.
- (15) Dauber-Osguthorpe, P.; Roberts, V. A.; Osguthorpe, D. J.; Wolff, J.; Genest, M.; Hagler, A. T. *Proteins: Struct., Funct., Genet.* **1988**, *4*, 31.
- (16) Rappe, A. K.; Bernstein, E. R. *J. Phys. Chem. A* **2000**, *104*, 6117.
- (17) Yin, D. X.; MacKerell, A. D. *J. Phys. Chem.* **1996**, *100*, 2588.
- (18) Yin, D. X.; Mackerell, A. D. *J. Comput. Chem.* **1998**, *19*, 334.
- (19) Chen, I. J.; Yin, D. X.; MacKerell, A. D. *J. Comput. Chem.* **2002**, *23*, 199.
- (20) Frisch, M. J.; Trucks, G. W.; Schlegel, H. B.; Scuseria, G. E.; Robb, M. A.; Cheeseman, J. R.; Zakrzewski, V. G.; Montgomery, J. A., Jr.; Stratmann, R. E.; Burant, J. C.; Dapprich, S.; Millam, J. M.; Daniels, A. D.; Kudin, K. N.; Strain, M. C.; Farkas, O.; Tomasi, J.; Barone, V.; Cossi,

- M.; Cammi, R.; Mennucci, B.; Pomelli, C.; Adamo, C.; Clifford, S.; Ochterski, J.; Petersson, G. A.; Ayala, P. Y.; Cui, Q.; Morokuma, K.; Malick, D. K.; Rabuck, A. D.; Raghavachari, K.; Foresman, J. B.; Cioslowski, J.; Ortiz, J. V.; Stefanov, B. B.; Liu, G.; Liashenko, A.; Piskorz, P.; Komaromi, I.; Gomperts, R.; Martin, R. L.; Fox, D. J.; Keith, T.; Al-Laham, M. A.; Peng, C. Y.; Nanayakkara, A.; Gonzalez, C.; Challacombe, M.; Gill, P. M. W.; Johnson, B. G.; Chen, W.; Wong, M. W.; Andres, J. L.; Head-Gordon, M.; Replogle, E. S.; Pople, J. A. *Gaussian 98*, revision A.9; Gaussian, Inc.: Pittsburgh, PA, 1998.
- (21) Becke, A. D. *J. Chem. Phys.* **1993**, *98*, 5648.
- (22) Lee, C.; Yang, W.; Parr, R. G. *Phys. Rev. B: Condens. Matter Mater. Phys.* **1988**, *37*, 785.
- (23) Hariharan, P. C.; Pople, J. A. *Theor. Chim. Acta* **1973**, *28*, 213.
- (24) Hehre, W. J.; Ditchfield, R.; Pople, J. A. *J. Chem. Phys.* **1972**, *56*, 2257.
- (25) Krishnan, R.; Binkley, J. S.; Seeger, R.; Pople, J. A. *J. Chem. Phys.* **1980**, *72*, 650.
- (26) Moller, C.; Plesset, M. S. *Phys. Rev.* **1934**, *46*, 618.
- (27) Pople, J. A.; Seeger, R.; Krishnan, R. *Int. J. Quantum Chem. Symp.* **1977**, *11*, 149.
- (28) Jorgensen, W. L.; Chandrasekhar, J.; Madura, J. D.; Impey, R. W.; Klein, M. L. *J. Chem. Phys.* **1983**, *79*, 926.
- (29) Brooks, B. R.; Bruccoleri, R. E.; Olafson, B. D.; States, D. J.; Swaminathan, S.; Karplus, M. *J. Comput. Chem.* **1983**, *4*, 187.
- (30) Fenclova, D.; Dohnal, V. *J. Chem. Thermodyn.* **1990**, *22*, 219.
- (31) Kale, L.; Skeel, R.; Bhandarkar, M.; Brunner, R.; Gursoy, A.; Krawetz, N.; Phillips, J.; Shinozaki, A.; Varadarajan, K.; Schulten, K. *J. Comput. Phys.* **1999**, *151*, 283.
- (32) Lide, D. R. *CRC Handbook of Chemistry and Physics*, 74th ed.; CRC Press: Boca Raton, 1993.
- (33) Secher, O. *Acta Anaesthesiol. Scand. Suppl.* **1971**, *42*, 1.
- (34) Essmann, U.; Perera, L.; Berkowitz, M. L.; Darden, T.; Lee, H.; Pedersen, L. G. *J. Chem. Phys.* **1995**, *103*, 8577.
- (35) Nose, S. *J. Chem. Phys.* **1984**, *81*, 511.
- (36) Hoover, W. G. *Phys. Rev. A: At., Mol., Opt. Phys.* **1985**, *31*, 1695.
- (37) Parra, R. D.; Zeng, X. C. *J. Fluorine Chem.* **1997**, *83*, 51.
- (38) Rothlisberger, U.; Laasonen, K.; Klein, M. L.; Sprik, M. *J. Chem. Phys.* **1996**, *104*, 3692.
- (39) Tsuzuki, S.; Uchimaru, T.; Tanabe, K.; Kuwajima, S. *J. Phys. Chem.* **1994**, *98*, 1830.
- (40) Watkins, E. K.; Jorgensen, W. L. *J. Phys. Chem. A* **2001**, *105*, 4118.
- (41) Majer, V.; Svoboda, V.; Eds. *International Union of Pure and Applied Chemistry Chemical Data Series, No. 32: Enthalpies of Vaporization of Organic Compounds*, 1985.
- (42) Nose, S.; Klein, M. L. *J. Chem. Phys.* **1983**, *78*, 6928.
- (43) Xu, Y.; Tang, P. *Biochim. Biophys. Acta* **1997**, *1323*, 154.
- (44) Roth, S. H.; Miller, K. W.; Eds. *Molecular and Cellular Mechanisms of Anesthetics [Based on the 3rd International Conference on Molecular and Cellular Mechanisms of Anesthesia, University of Calgary, June 13–15, 1984]*, 1986.